Science Advances

AAAS

advances.sciencemag.org/cgi/content/full/1/11/e1500849/DC1

Supplementary Materials for

Bioinspired large-scale aligned porous materials assembled with dual temperature gradients

Hao Bai, Yuan Chen, Benjamin Delattre, Antoni P. Tomsia, Robert O. Ritchie

Published 11 December 2015, *Sci. Adv.* **1**, e1500849 (2015)
DOI: 10.1126/sciadv.1500849

The PDF file includes:

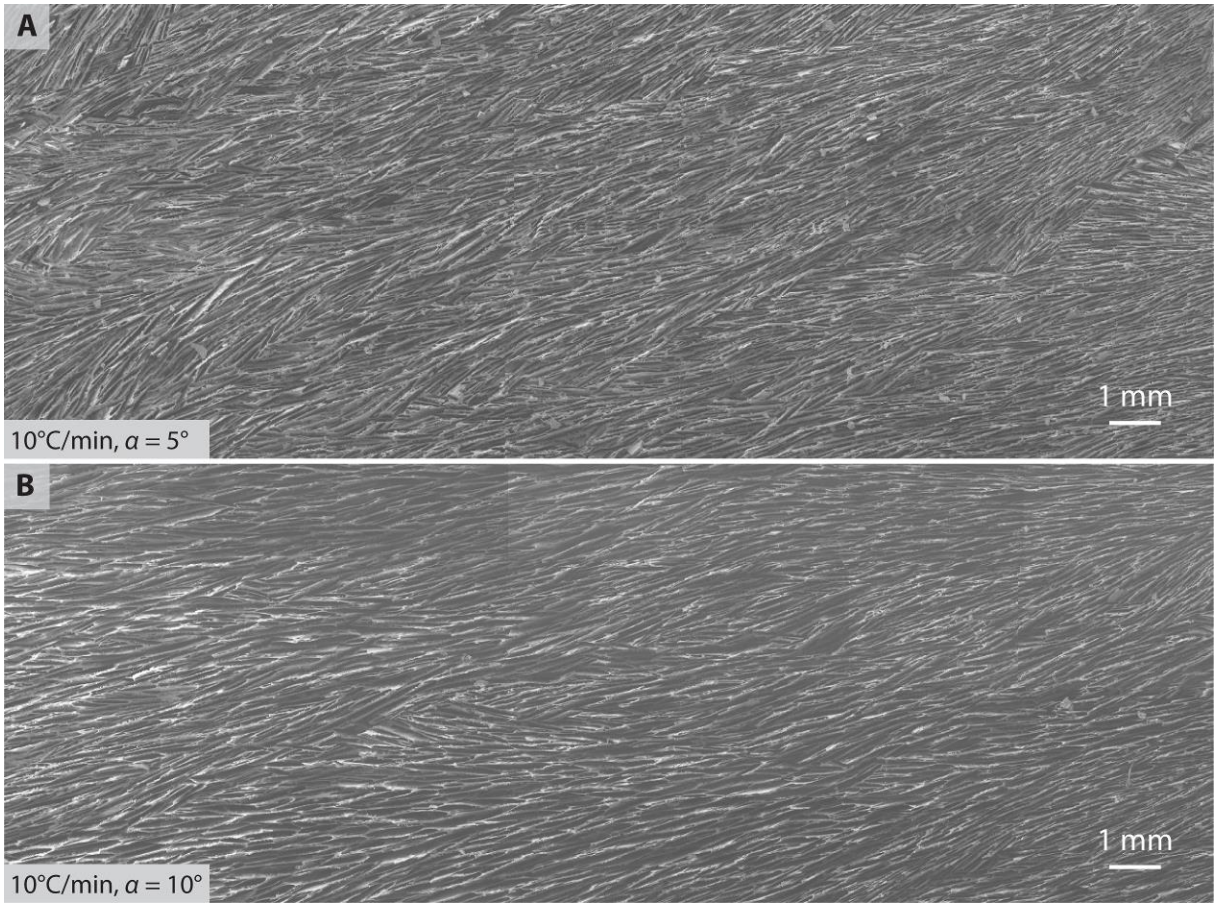

Figure S1. Representative SEM image of HA scaffold prepared by bidirectional freezing in the cross section perpendicular to the cold finger. Both samples were prepared at 10°C/min but with different slope angle: (**A**) α = 5°, (**B**) α = 10°, respectively. Both samples show large-scale lamellar structure.

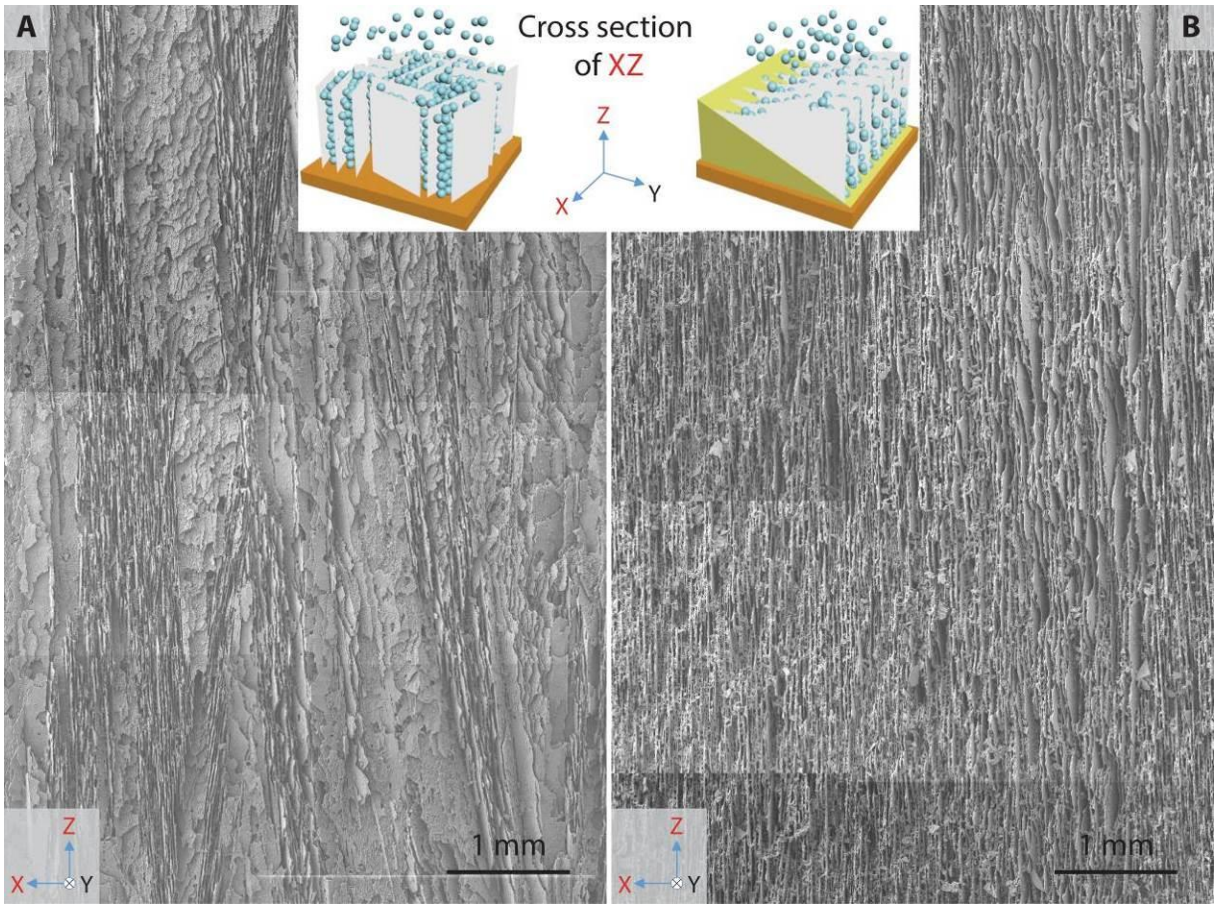

Figure S2. Representative SEM image of HA scaffold in the cross section perpendicular to the cold finger. Samples were prepared by (**A**) conventional and (**B**) bidirectional freezing, respectively. (**A**) As ice crystals only grow under the vertical temperature gradient, lamellar structure has many domains with different orientation. (**B**) As ice crystals grow under dual temperature gradients, lamellar structure has only one domain that aligns along the wedge. The samples were both prepared with a 20 vol.% HA slurry, using a cooling rate of 10°C/min. A PDMS wedge (α = 20°) was used for bidirectional freezing.

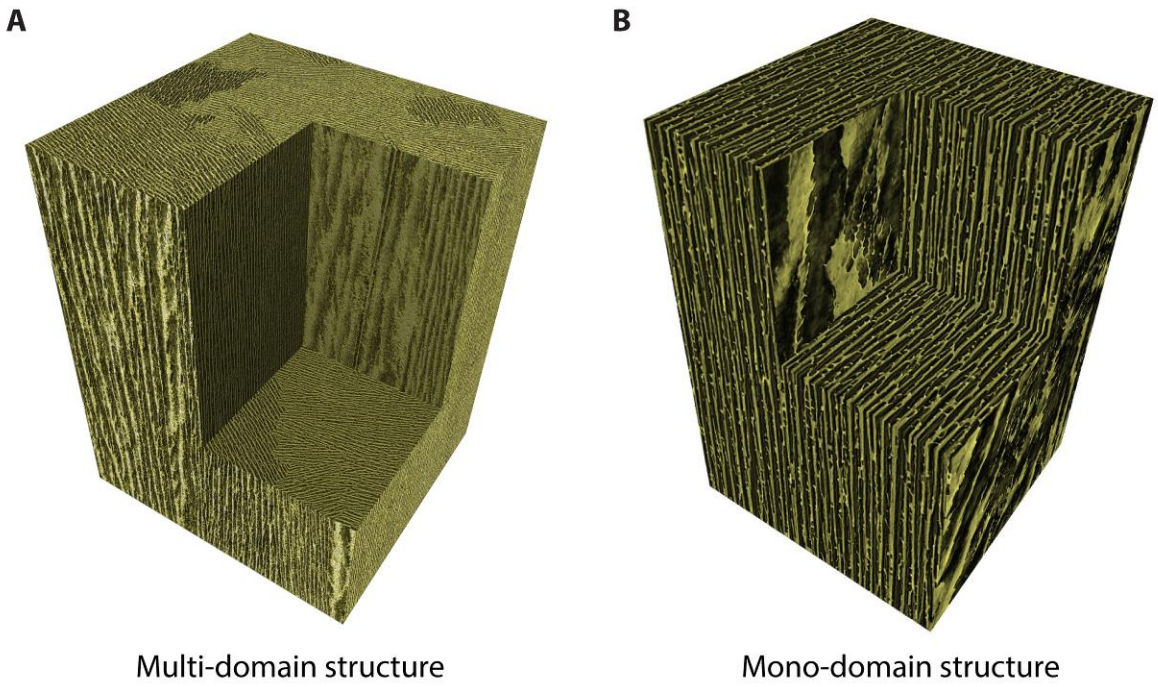

Figure S3. X-ray computed microtomography images for scaffolds prepared by (A) conventional and (B) bidirectional freezing. (**A**) The scaffold prepared by conventional freezing shows a multi-domain structure. Sample size: 1.6 x 1.5 x 2 mm. (**B**) The scaffold prepared by bidirectional freezing shows a mono-domain structure. Sample size: 1 x 1 x 1.5 mm.

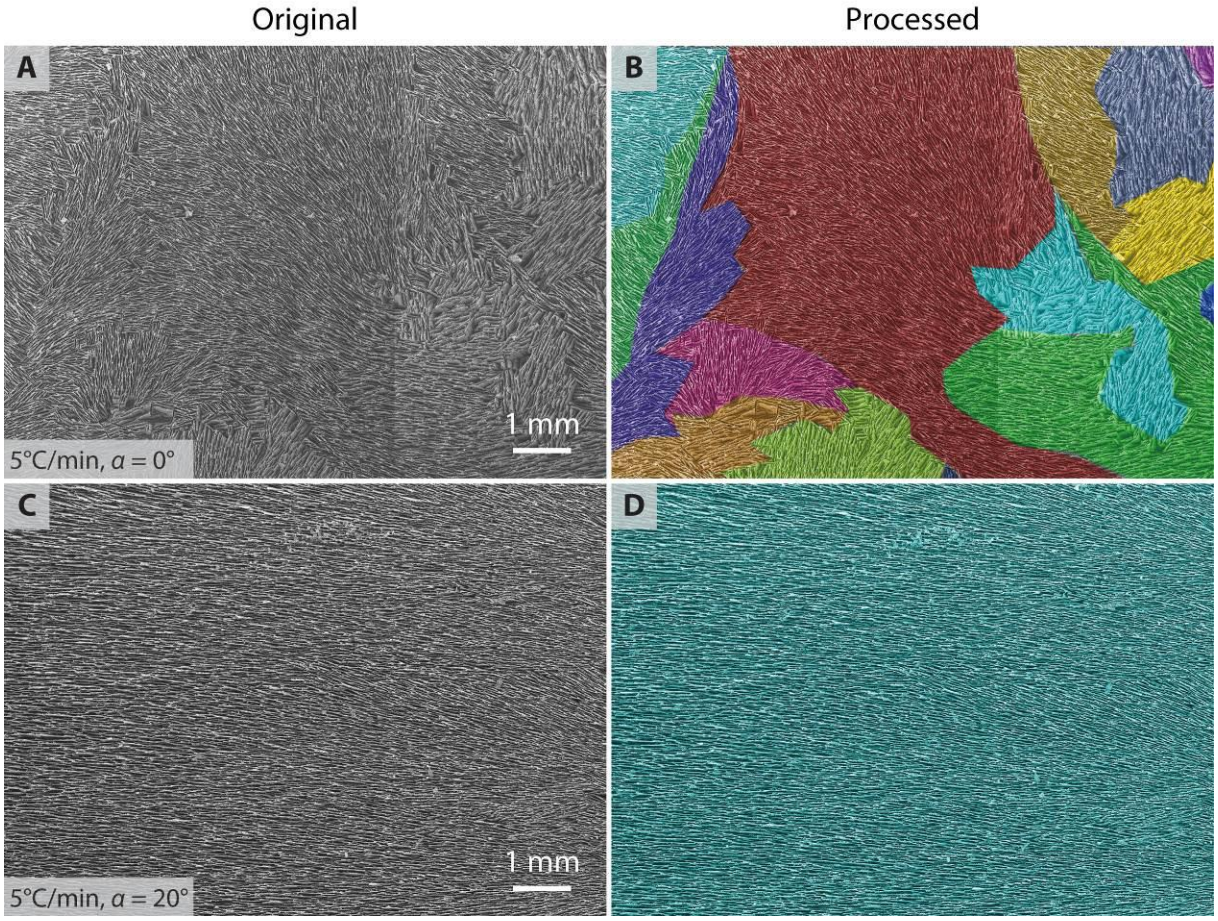

Figure S4. Processing of SEM images. (**A**, **C**) Original SEM images of scaffolds cross-sections. (**B**, **D**) Processed SEM images: domains were artificially colored based on their orientations. This clearly shows the difference in domain numbers for (**A** and **B**) conventional and (**C** and **D**) bidirectional freeze-casting.

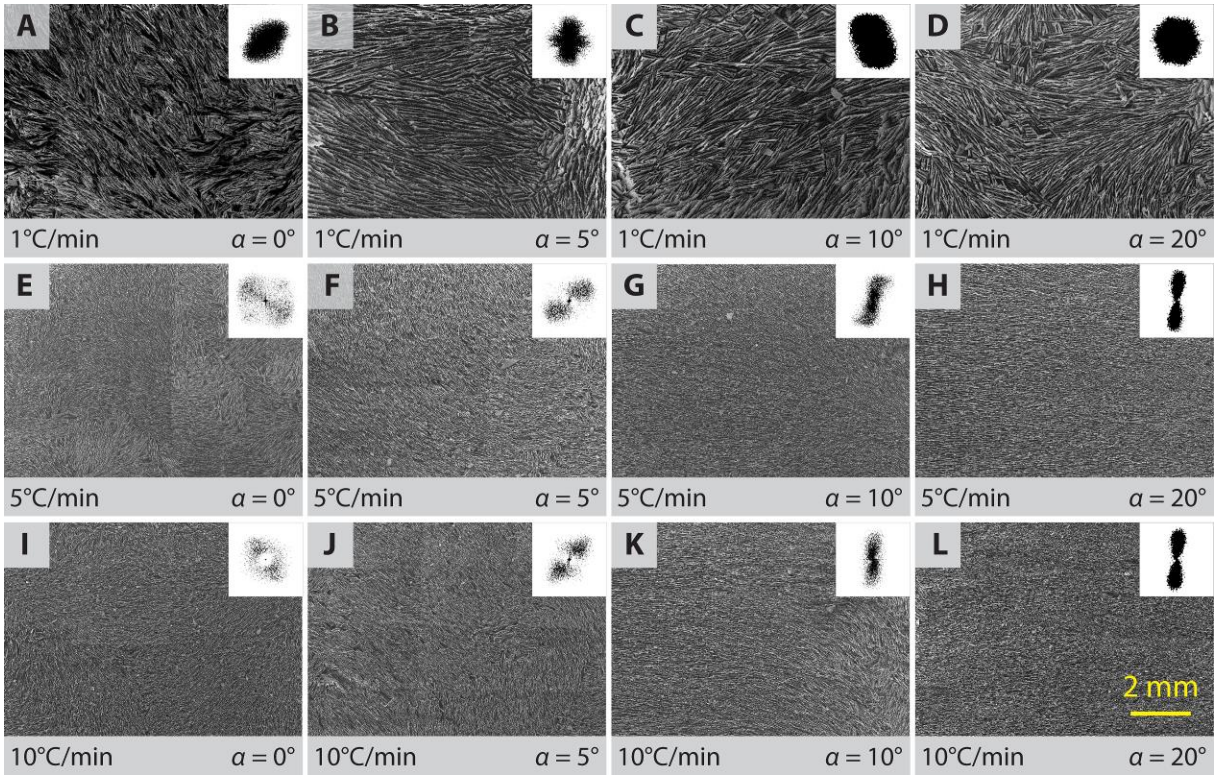

Figure S5. Original SEM images of samples prepared under various conditions. For slope angles of 10° and 20°, a large single domain can be observed across the whole sample length.

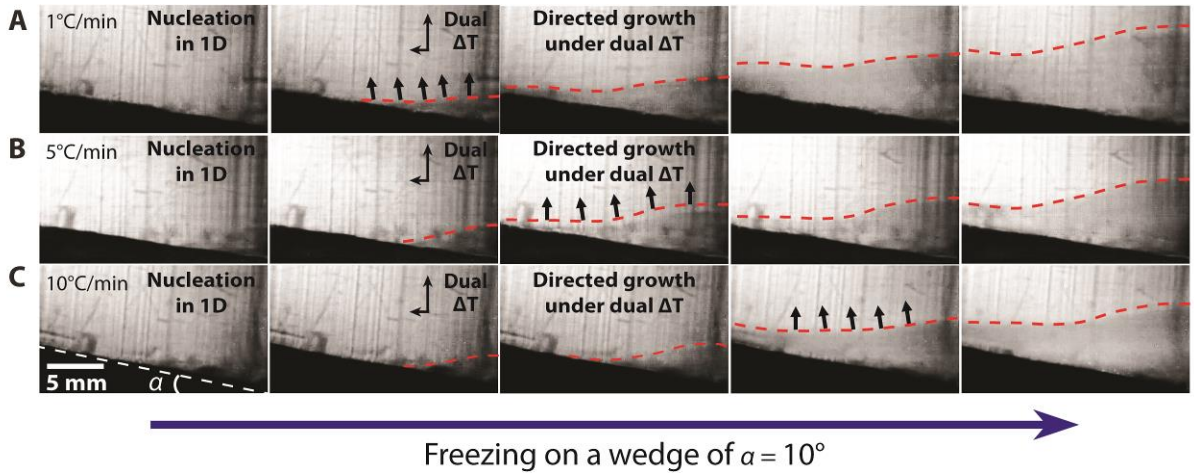

Figure S6. Optical images showing ice profiles during freeze casting under dual temperature gradients with α = 10°, but at different cooling rates. (**A**) 1°C/min, (**B**) 5°C/min, (**C**) 10°C/min. Gradient nucleation and wavy ice profiles were observed under all these cooling rates.

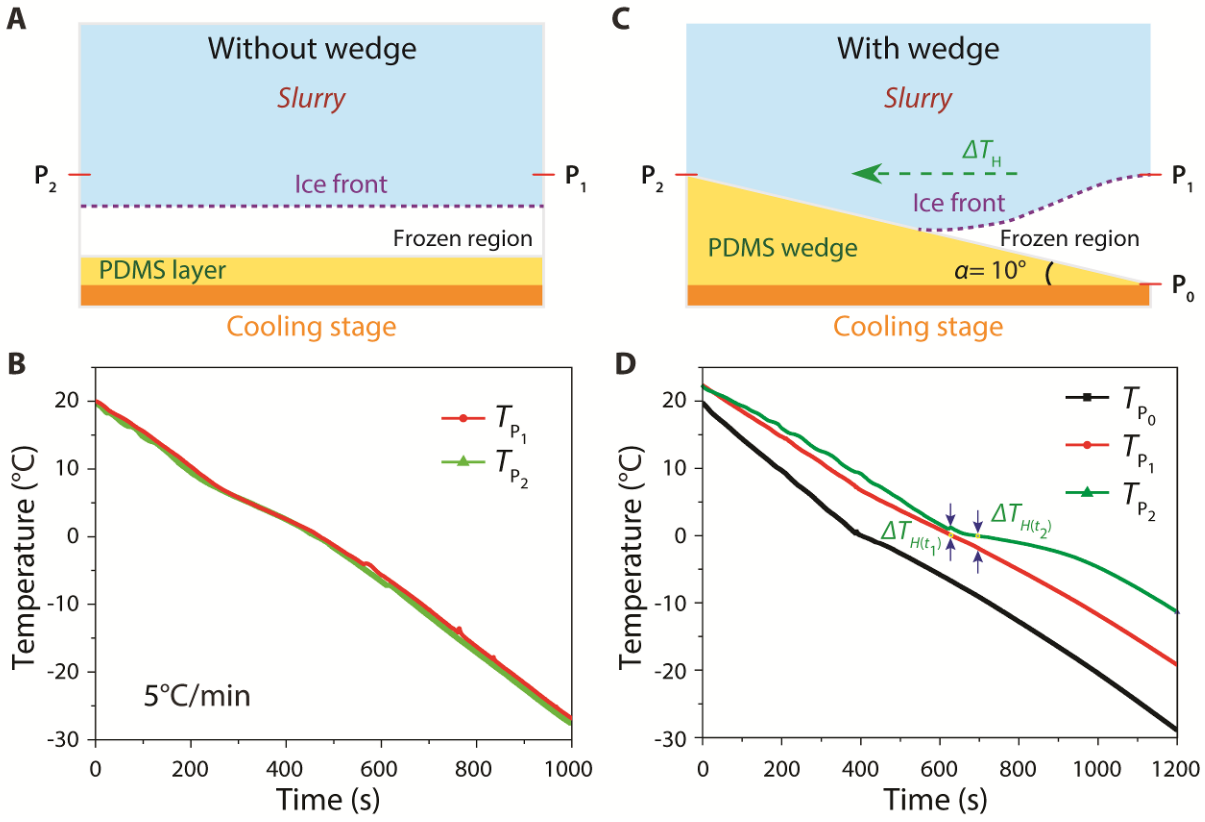

Figure S7. Temperature measurements during conventional and bidirectional freeze casting. Thermocouples were used to record the slurry temperature *in situ* at specific positions. (**A**) When a uniform PDMS film (~ 1 mm thickness) was used, the slurry nucleated simultaneously over the entire substrate. This resulted in an ice profile that remained flat during the entire freezing process. (**B**) The superposition of the two temperatures profiles, recorded at positions P_1 and P_2, further confirmed the presence of a single vertical temperature gradient. (**C**) A PDMS wedge with a slope angle of 10° generated a wavy ice profile. (**D**) A temperature shift is observed between positions P_1 and P_2, indicating that a horizontal temperature gradient was generated by the wedge.

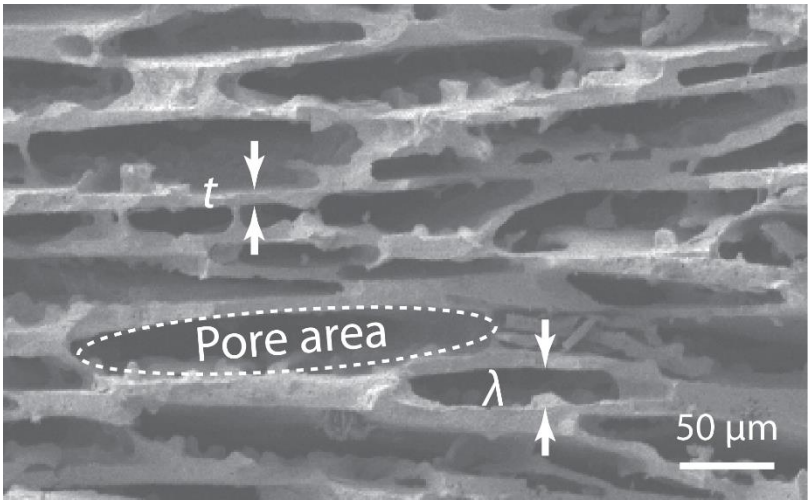

Figure S8. Representative SEM image of the cross section of a freeze-cast HA scaffold illustrating the different structural features and parameters. Lamellae thickness (t), interlamellar spacing (λ) and pore area (A_p) are indicated. The sample was prepared by bidirectional freeze-casting from a 20 vol.% HA slurry, using a cooling rate of 5°C/min and a PDMS wedge with an angle of α = 20°.

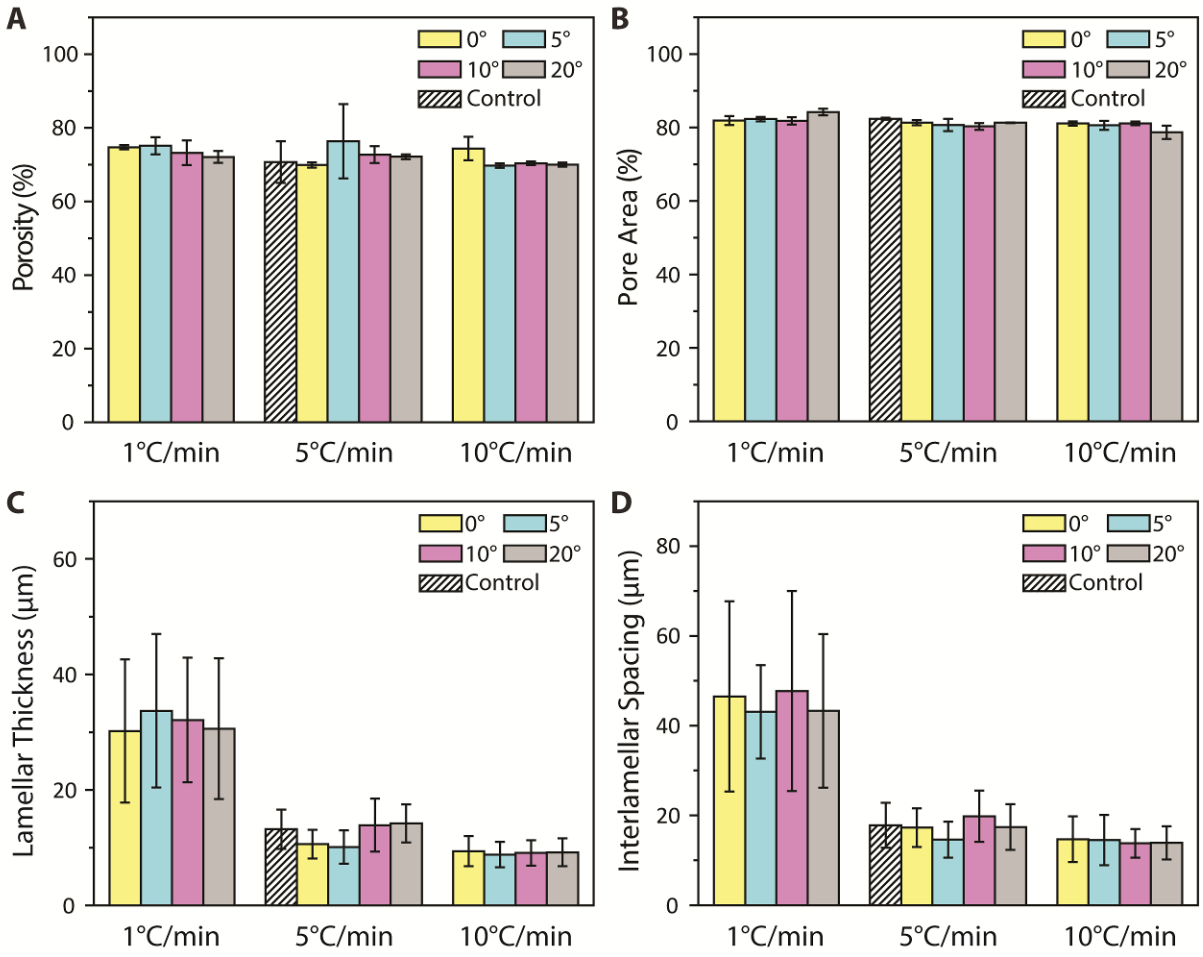

Figure S9. Structural parameters of HA scaffolds fabricated by bidirectional freezing. Structural parameters such as (**A**) porosity (φ), (**B**) pore area (A_p), (**C**) lamellae thickness (t) and (**D**) interlamellar spacing (λ) were measured from SEM images. For all samples, a change in cooling rate or slope angle did not affect the sample porosity or the pore area. However, both the lamellae thickness and interlamellar spacing markedly decreased with increase in cooling rate. Eventually, at a given cooling rate, no obvious difference was observed between samples prepared by conventional (referred here as 'control') and bidirectional freeze-casting.

Table S1. Porosity, pore area, lamellae thickness, interlamellar spacing, compressive strength, and Young's modulus values for scaffolds prepared with different cooling rates (1, 5, and 10°C/min) and slope angles (0°, 5°, 10°, and 20°).

Cooling rate	Slope angle	Porosity φ (%)	Pore Area A_p (%)	Lamellar thickness t (μm)	Interlamellar spacing, λ (μm)	Strength (MPa)	Modulus (MPa)
1°C/min	control	---	---	---	---	1.9±0.1	59.1±3.3
1°C/min	0°	74.7±0.6	81.9±1.2	30.2±12.4	46.5±21.2	2.7±0.1	62.3±7.8
1°C/min	5°	75.1±2.3	82.3±0.6	33.7±13.3	43.1±10.4	2.4±0.2	77.0±0.5
1°C/min	10°	73.2±3.3	81.8±1.0	32.1±10.8	47.7±22.3	2.1±0.7	72.2±13.7
1°C/min	20°	72.1±1.6	84.2±0.9	30.6±12.2	43.3±17.1	1.5±0.4	44.4±16.9
5°C/min	control	70.7±5.6	82.4±0.3	13.2±3.4	17.8±5.0	9.5±1.0	189.2±23.1
5°C/min	0°	69.9±0.7	81.3±0.7	10.6±2.5	17.3±4.3	8.9±1.7	234.9±52.5
5°C/min	5°	76.3±10.1	80.7±1.7	10.1±2.9	14.6±4.0	9.5±1.5	181.7±42.9
5°C/min	10°	72.7±2.2	80.3±0.9	13.9±4.6	19.8±5.7	8.7±1.9	236.7±53.0
5°C/min	20°	72.1±0.6	81.3±0.1	14.2±3.3	17.4±5.1	4.9±0.2	134.5±61.9
10°C/min	control	---	---	---	---	13.3±0.1	207.9±20.3
10°C/min	0°	74.3±3.1	81.1±0.6	9.4±2.6	14.7±5.1	10.6±1.2	235.8±42.8
10°C/min	5°	69.7±0.6	80.6±1.2	8.8±2.2	14.5±5.6	13.2±2.0	239.5±68.1
10°C/min	10°	70.4±0.5	81.1±0.5	9.1±2.2	13.8±3.2	11.2±2.4	202.7±47.2
10°C/min	20°	70.0±0.5	78.7±1.8	9.2±2.4	13.9±3.7	8.3±0.7	249.0±15.4

Table S2. Compressive strength and Young's modulus values for scaffolds prepared by conventional (control) and bidirectional (α = 20°) freezing, both at 10°C/min. Samples were compared in X, Y, and Z axis.

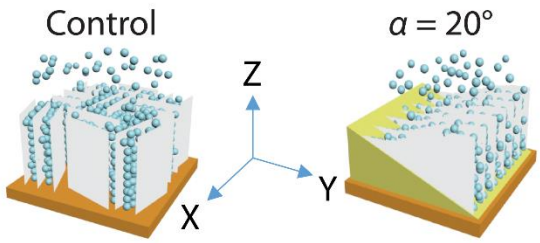

Cooling rate	Slope angle	Axis	Strength (MPa)	Modulus (MPa)
10°C/min	control	X	2.27 ±0.7	13.4±3.6
10°C/min	control	Y	1.76±0.8	19.3±1.4
10°C/min	control	Z	13.3±0.1	207.9±20.3
10°C/min	20°	X	1.06±0.6	15.59±4.1
10°C/min	20°	Y	6.53±0.7	182.6±19.8
10°C/min	20°	Z	8.3±0.7	249.0±15.4